Int. J. Electrochem. Sci., 7 **(2012)** 11149 - 11160

International Journal of
ELECTROCHEMICAL
SCIENCE
www.electrochemsci.org

The Inhibition Effect of Bis-Benzimidazole Compound For Mild Steel in 0.5 M HCl Solution

Xiumei Wang

School of Materials Science and Engineering, Shenyang Jianzhu University, Shenyang 110168, China
*E-mail: xmwang@alum.imr.ac.cn

Received: 17 September 2012 / *Accepted:* 13 October 2012 / *Published:* 1 November 2012

The compound BBMB was synthesized from the dehydration reaction o-phenylenediamine and 1, 4-benzendicarboxylic acid in polyphosphoric acid. The effectiveness of BBMB as corrosion inhibitor for mild steel in 0.5 M HCl solution was investigated by various techniques such as weight loss measurement, potentiodynamic polarization, electrochemical impedance spectroscopy (EIS). The results of these investigations showed enhancement in inhibition efficiencies with the increase in BBMB concentration and even at the concentration 0.01 mM the *IE*% exceeded 80%. BBMB suppressed both mild steel dissolution and hydrogen reduction processes acting as a mixed-type inhibitor. The excellent inhibition effectiveness of BBMB was also verified by scanning electron microscope (SEM). BBMB precluded mild steel corrosion by blocking the active sites on mild steel surface. The adsorption of BBMB on mild steel surface obeyed Langmuir adsorption isotherm**.**

Keywords: Mild Steel; Electrochemical Technique; SEM; Corrosion Inhibitor

1. INTRODUCTION

A number of organic compounds are known to be applicable as corrosion inhibitors for metal in acidic environments such as acid pickling, industrial acid cleaning, acid descaling and oil well acidizing. Such compounds typically contain nitrogen, oxygen, phosphorus or sulphur in a conjugated system and function via adsorption of the molecules on the metal surface, creating a barrier against corrodent attack [1-5]. Inhibition appears to be the result of adsorption of molecules and ions on the metal surface [5]. Adsorption can be described by two main types of interaction as follows: (a) Physisorption, involves electrostatic forces between ionic charges or dipoles on the adsorbed species and the electric charge at metal/solution interface. In this case, the heat of adsorption is low and therefore this type of adsorption is stable only at relatively low temperature. (b) Chemisorption, involves charge sharing or charge transfer from the inhibitor molecules to the metal surface to form a

coordinate type bond. In fact, electron transfer is typically for transition metals having vacant low-energy electron orbital. Chemisorption is typified by much stronger adsorption energy than physical adsorption. Such a bond is therefore more stable at higher temperatures [6-7]. The adsorption of these molecules depends mainly on certain physicochemical properties of the inhibitor molecule such as functional groups, steric factor, aromaticity, electron density at the donor atoms and p orbital character of donating electrons and electronic structure of the molecules [8-11].

Benzimidazole molecule shows two anchoring sites suitable for surface bonding: the nitrogen atom with its lonely sp^2 electron pair and the aromatic rings to facilitate the adsorption of compounds on the metallic surface [12]. Therefore, benzimidazole and its derivatives have received considerable research as excellent inhibitors for metals and alloys in acidic solution [9, 13-20]. However, the compounds bearing two benzimidazole rings as corrosion inhibitor have been rarely reported, and there is not adequate information available to profoundly understand their inhibition mechanism as acidic inhibitor.

In continuation of work on the acid corrosion inhibitors [21-24] 1, 4-bis (benzimidazolyl)-benzene (BBMB) was used as corrosion inhibitor for mild steel in 0.5 M HCl solution. Weight loss measurements, electrochemical impedance spectroscopy (EIS) and potentiodynamic polarization methods were employed to evaluate corrosion inhibition efficiency of the inhibitor. The mild steel surface was also examined by scanning electron microscopy (SEM). The adsorption of BBMB on mild steel surface was found to conform to the Langmuir isotherm with the negative adsorption free energy of -42.4 kJ mol^{-1}.

2. EXPERIMENTAL

2.1. Preparation of electrodes

The working electrode was a cylindrical disc cut from mild steel specimen with following chemical composition (wt): C (0.15%), Si (0.06%), Mn (0.32%), P (0.05%), and Fe (remainder). The mild steel disc with an area of 0.785 cm^2 was coated with epoxy except the working surface. The surface of working electrode was mechanically abraded using different grades of emery papers, which ended with the 800 grade, prior to use. The disc was cleaned by washing with bi-distilled water, acetone, respectively, and finally dried with a filter paper, then stored in the vacuum desiccators. For each test, a freshly abraded electrode was used.

2.2. Test solutions

The compound BBMB was synthesized from the dehydration reaction of 0.2 mol o-phenylenediamine and 0.1 mol 1, 4-benzendicarboxylic acid in polyphosphoric acid according to the published method [25]. The corrosion tests were performed in 0.5 M HCl solution in absence and presence of various BBMB concentrations, respectively. The concentrations of BBMB employed were 0.01, 0.02, 0.08, 0.16 mM. The test solutions were prepared from reagent grade HCl and bi-distilled

water. During the tests, the temperature of solutions was controlled at 298 K by using a water thermostat and the experiments were performed under static conditions.

2.3. Weight loss measurements

The mild steel sheets of 2.0 cm ×2.0 cm × 0.5 cm were abraded by different grades of emery paper (grade 100-800) and then washed with distilled water and acetone. After weighing accurately by digital balance with sensitivity of ±0.1 mg, the specimens were allowed to stand in beaker containing 250 mL 0.5 M HCl without and with different concentrations of BBMB using glass hooks and rods for 5h. All the aggressive acid solutions were open to air. Parallel triplicate experiments were performed and the average value of the weight loss was obtained. The corrosion rates (*r*) were calculated using the following equation [26]:

$$r_{\text{corr}} = \frac{W_1 - W_2}{St} \qquad (1)$$

where r_{corr} was the corrosion rate in (mg cm^{-2} h^{-1}), W_1 and W_2 were the average weight loss of three parallel mild steel sheets before and after immersion in corrosion media, respectively. *S* was the total area of one mild steel specimen, and *t* was immersion time (5 h). With the calculated corrosion rate, the inhibition efficiency (*IE* %) was calculated as follows [27-28]:

$$IE\% = 100 \times (r^0 - r_{\text{inh}}) / r^0 \qquad (2)$$

where $r^0$and r_{inh} were corrosion rates of mild steel in uninhibited and inhibited solutions, respectively. The specimens were immersed in the solutions without blocking any side, and the whole specimen area was considered in the calculation.

2.4 Electrochemical measurements

Electrochemical experiments were carried out using a standard electrochemical three electrode cell with a platinum counter electrode (CE) and a saturated calomel electrode (SCE) coupled to a fine Luggin capillary as the reference electrode. To minimize ohmic contribution, the Luggin capillary was close to working electrode (WE). Before measurement the electrode was immersed in test solution at open circuit potential (OCP) for 0.5 h until a steady state was reached. All electrochemical measurements were carried out using PARSTAT 2273 advanced electrochemical system (Princeton Applied Research). Electrochemical impedance spectroscopy measurements were performed at OCP over a frequency range of 100 kHz to 0.01 Hz with a signal amplitude perturbation of 10 mV. *IE*% is defined as:

$$IE\% = \frac{R_{p(inh)} - R_p}{R_{p(inh)}} \times 100\% \qquad (3)$$

where R_p and $R_{p\ (inh)}$ were the values of polarization resistance in the absence and presence of inhibitor, respectively [29].

The potentiodynamic polarization curves were performed with a scan rate of 0.5 mV s^{-1} in the potential range from -150 to + 250 mV vs. corrosion potential (E_{corr} vs. SCE). *IE*% is defined as:

$$IE\% = \frac{I_{corr} - I_{corr}^{inh}}{I_{corr}} \times 100\% \qquad (4)$$

where I_{corr} and I_{corr}^{inh} represented corrosion current densities in the absence and presence of an inhibitor, respectively [30], determined by extrapolation of Tafel lines to the corrosion potential.

2.5 Surface morphology analysis

The surface morphologies of the mild steel samples with dimension 2.0 cm ×2.0 cm×0.5 cm prepared as described above (Sect. 2.3) after immersion in 0.5 M HCl solution without and with 0.16 mM BBMB at 298K for 5 h, were investigated by SEM using a PHILIPS model XL30 microscope.

3. RESULTS AND DISCUSSION

3.1. Weight loss measurements

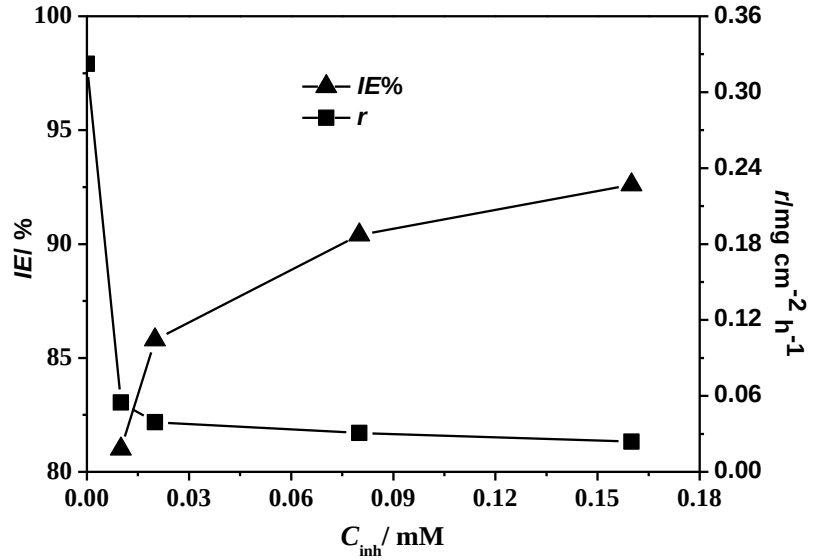

Figure 1. Inhibition efficiency and corrosion rate of mild steel in 0.5 M HCl solution without and with different concentration of BBMB obtained from Weight loss.

Fig. 1 shows the corrosion rates of mild steel in 0.5 M HCl solution without and with different concentrations of BBMB. The corrosion rates decrease noticeably with the increase in BBMB concentration from 0.01 to 0.16 mM of BBMB, respectively. The inhibition efficiency as a function of concentrations of prepared inhibitor BBMB was also calculated and shown in Fig. 1. The corrosion inhibition enhances with the inhibitor concentration.

This behavior is due to the fact that the adsorption coverage of inhibitor on mild steel surface increases with the inhibitor concentration [31]. When the concentration of BBMB is less than 0.08 mM, *IE*% increases sharply with increase in concentration, while a further increase causes no appreciable change in performance. The maximum *IE*% is 92.6% at 0.16 mM and the inhibition is estimated to be higher than 80% even at 0.01 mM which indicates that BBMB is a very good inhibitor for mild steel in 0.5 M HCl solution.

3.2. Electrochemical impedance

The impedance spectra for mild steel in 0.5 M HCl solution without and with various concentrations of BBMB are presented as Nyquist plots in Figs. 2. From these plots, the impedance response of mild steel has significantly changed on addition of the BBMB. For analysis of the impedance spectra containing a depressed capacitive semi circle [32], the standard Randle circuit is shown in Fig.3 [33-34].

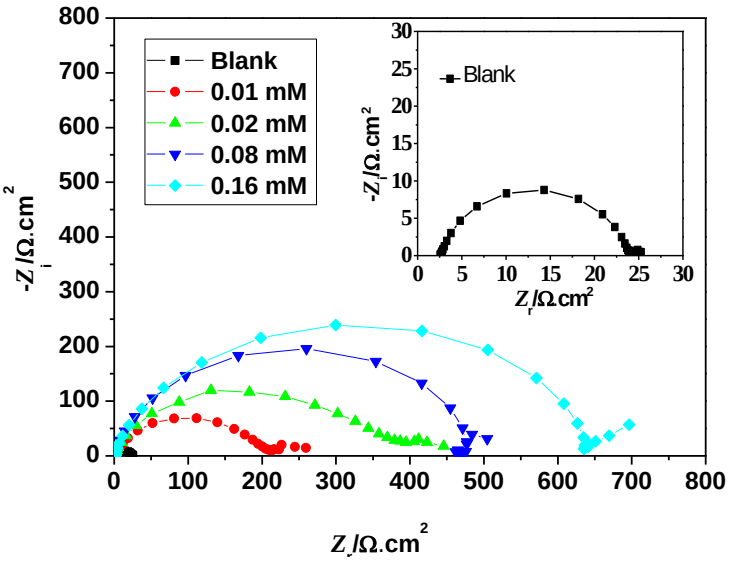

Figure 2. Nyquist plots of mild steel electrode obtained in 0.5 M HCl solution without and with different concentration of BBMB.

The depression in Nyquist semicircles is a feature for solid electrodes and often referred to as frequency dispersion and attributed to the roughness and other inhomogenities of the solid electrode

[35-36]. C_{dl} is replaced by a constant phase element (CPE) with the exponent, n. It is found that the Nyquist plots for various concentrations of BBMB inhibitor showed similar trend of curves which was depressed semicircle with the centre located below the real X-axis. Increasing the inhibitor concentration will increase the size of the curves, indicating the time constant of the charge transfer and double-layer capacitance [18]. This behaviour shows the adsorption of BBMB on mild steel surface.

It is also found that from the Nyquist plots, even with the addition or absence of inhibitor does not alter the style of impedance curves, thus proposing a similar mechanism of inhibition is involved. The impedance parameters derived from these plots are given in Table 1. As noted from Table 1, the polarization resistances values containing inhibitor substantially increased along the concentration compared to that without inhibitor. It is also clear that the value of C_{dl} decreases on the addition of inhibitors, indicating a decrease in the local dielectric constant and/or an increase in the thickness of the electrical double layer, suggesting the inhibitor molecules function by the formation of the protective layer at the metal surface.

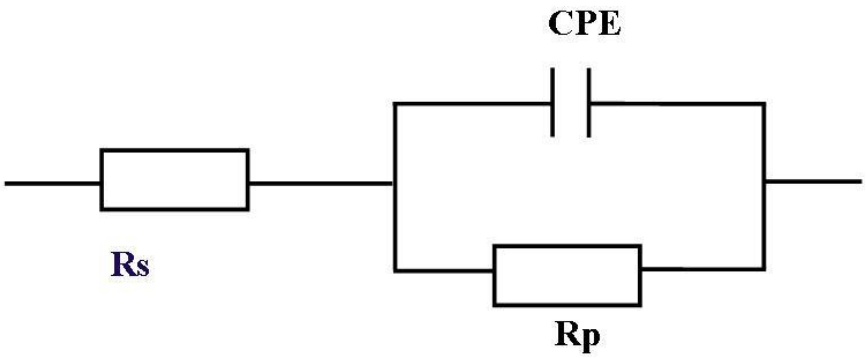

Figure 3. the standard Randle circuit

Table 1. Data from electrochemical impedance spectroscopy measurements of mild steel in 0.5 M HCl solution in the absence and presence of various concentrations of BBMB.

C_{inh}	R_s	*CPE*	R_p	*IE*
/ mM	/ Ω cm^2	/ μF cm^{-2}	/ Ω cm^2	/ %
Blank	2.81	133.7	21	-
0.01	1.65	51.3	215	90.2
0.02	1.55	37.2	379	94.5
0.08	1.62	19.2	474	95.6
0.16	1.34	18.8	640	96.7

3.3.1. Potentiodynamic polarization

Fig. 4 shows the potentiodynamic polarization curves after the addition of corrosion inhibitor BBMB. In every curve, it is observed that the current densities of the anodic and cathodic branch are displaced towards lower values. This displacement is more evident with the increase in concentration

of the corrosion inhibitor when compared to the blank material. From Fig. 4, it can be seen that, the inhibitor begins to desorb at a potential closer to -350 mV/SCE at 0.16 mM, which can be called as desorption potential. The desorption potential is the symbol of inhibition effect. The desorption potential increases with the inhibitor concentration which indicates that the inhibition effect enhanced with the increase in the inhibitor concentration. The similar behaviour has been obtained with other researches [23, 37].

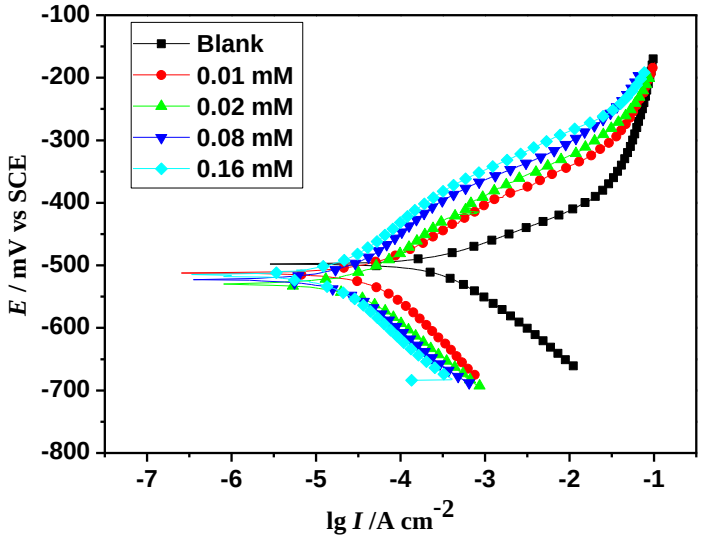

Figure 4. Potentiodynamic polarization plots of mild steel electrode obtained in 0.5 M HCl solution without and with different concentration of BBMB.

Table 2. Data obtained from potentiodynamic polarization measurements of mild steel immersed in 0.5 M HCl solution in the absence and presence of various concentrations of BBMB.

C_{inh}	E_{corr}	I_{corr}	β_a	β_c	*IE*
/ mM	/mV	/mA cm^{-2}	/mV	/mV	%
Blank	-499	0.37	67.7	110.7	-
0.01	-512	0.056	82.5	132.6	84.9
0.02	-520	0.037	95.6	121.6	90.0
0.08	-522	0.029	113.2	128.0	92.2
0.16	-516	0.012	102.5	122.3	96.8

The corrosion parameters extracted from polarisation curves containing corrosion current density (I_{corr}), corrosion potential (E_{corr}), the anodic and cathodic Tafel slopes (β_a, β_c), inhibition efficiency (*IE*%) have been calculated as a function of BBMB concentration according to equation (4) [30, 38-39] and have been presented in Table 2. From table 2, the corrosion current density decreased with the increase of the inhibitor concentration and *IE*% showed the opposite trend which indicated

that the inhibitor suppressed the mild steel corrosion in 0.5 M HCl solution. The presence of BBMB resulted in no definite trend in the shift of E_{corr} compared to that in the absence of BBMB, however, the displacement in E_{corr} is < 85 mV. These results indicated that the presence of BBMB inhibited both iron oxidation and hydrogen evolution, consequently BBMB can be classified as mixed corrosion inhibitor [40-42] with the inhibitory action caused by a geometric blocking effect [43]. In addition, the inhibitory action was due to a reduction of the reaction area on the surface of the corroding metal [44]. It is important to note that there exists a difference in corrosion efficiency between weight loss tests and electrochemical method, although the inhibition tendency is similar at 298 K in both tests, probably because the former was performed for a longer time (5 h) than the latter (after reaching OCP, 0.5 h).

3.4 Adsorption isotherm

Adsorption isotherms provide information about the interaction among the adsorbed molecules themselves and also their interactions with the electrode surface which is influenced by the chemical structures of organic compounds, the nature and surface charge of metal, the distribution of charge in molecule and the type of aggressive media. Adsorption isotherms were established to describe the adsorption behaviour of the studied corrosion inhibitor on mild steel surface. Several adsorption isotherms are attempted to fit the surface coverage θ, including Frumkin, Temkin, Freundlich and Langmuir isotherms. For the studied inhibitors, it is found that the experimental data obtained from weight loss measurements, as an example of the other used experimental techniques, could fit the Langmuir adsorption isotherm. According to this isotherm, the surface coverage (θ) ($\theta=(r^0-r_{inh})/r^0$) is related to inhibitor concentration, C_{inh}, by the relation [45-47]:

$$\theta/(1-\theta) = K_{ads}C_{inh} \quad (5)$$

Where K_{ads} is the adsorption equilibrium constant. Experimental results of C_{inh}/θ vs. C_{inh} yielded straight lines as shown in Fig. 5 and the value of the correlation coefficient and the adsorption equilibrium constant are given in Table 3. The linear correlation coefficient (r) is almost equal to 1 (r = 0.99986) and the slope is very close to 1 (slope = 1.0727), indicating the adsorption of BBMB on mild steel surface obeys Langmuir adsorption isotherm. The adsorptive equilibrium constant (K_{ads}) value is calculated from the reciprocal of the intercept of 0.00161 mM as 6.21×10^5 M^{-1}. Adsorption isotherms are important as equilibrium constant lead to standard free energy of adsorption [48]:

$$\Delta G^0_{ads} = -RT\ln(55.5K_{ads}) \quad (6)$$

Where θ is coverage degree of BBMB on the mild steel surface, K_{ads} is the equilibrium constant, R is 8.314 J mol^{-1} K^{-1} mol^{-1}, T is 298 K, ΔG^0_{ads} is the adsorption free energy which reflects a spontaneous capacity of inhibitor molecule adsorbed on the surface of the metal. It has been reported that the absolute value of ΔG^0_{ads} up to 20 kJ mol^{-1} or lower indicates a physical adsorption between the

charged molecules and metal [49], while that more negative than -40 kJ mol^{-1} involves sharing or transfer of electron from the inhibitor molecules to the metal surface to form a coordinate type bond (chemisorption) [37, 50]. The calculated ΔG^0_{ads} value was -42.4 kJ mol^{-1} which shows that BBMB adsorbed on the surface of mild steel through chemisorption. It should be noted that, the adsorption phenomenon of an organic molecule is not considered only as a physical or as a chemical adsorption phenomenon. BBMB is an organic base; it can be protonated in the acid solution. Cl^- ions could accumulate gradually close to the steel/solution interface, being specifically adsorbed; they create an excess negative charge towards the solution and favor more adsorption of the cations, then protonated BBMB may adsorb through electrostatic interactions between the positively charged molecules and the negatively charged metal surface and chemisorption. Chemical adsorption of BBMB arises from the donor acceptor interactions between free electron pairs of N and p electrons of multiple bonds and vacant d orbitals of iron [41, 51]. It has been reported that [52] the adsorption of heterocyclic compounds occurs with the aromatic rings sometimes parallel but mostly normal to the metal surface.

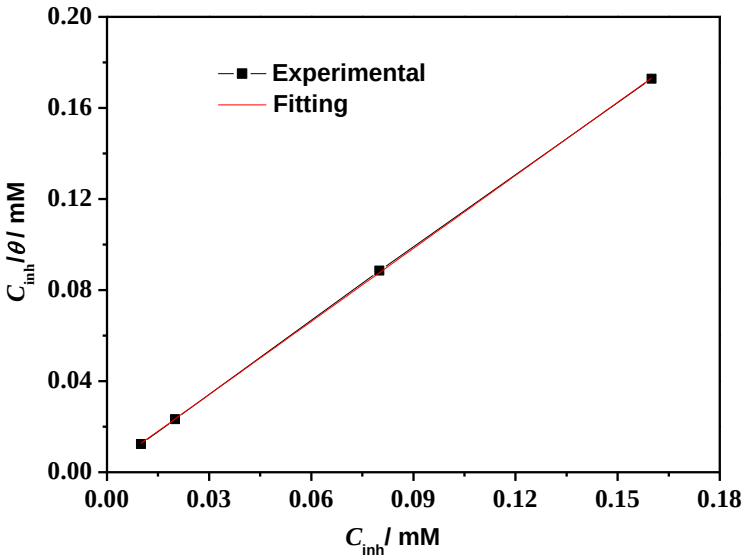

Figure 5. The plot of C_{inh}/θ vs. C_{inh}.

Table 3. Thermodynamic parameters for BBMB as corrosion inhibitor of mild steel in 0.5 M HCl solution.

inhibitor	K_{ads}	$\Delta_r G^0_{ads}$	slope	intercept	correlation coefficient (r)
	/$\times 10^5$ M^{-1}	/kJ.mol^{-1}		mM	
BBMB	4.95	42.4	1.070	0.00202	0.9999

3.5 Surface morphology observation

The SEM images of mild steel in 0.5 M HCl solution in the absence and presence of 0.16 mM BBMB after 5 h immersion are taken and observed in order to support our findings and shown in Fig. 6.

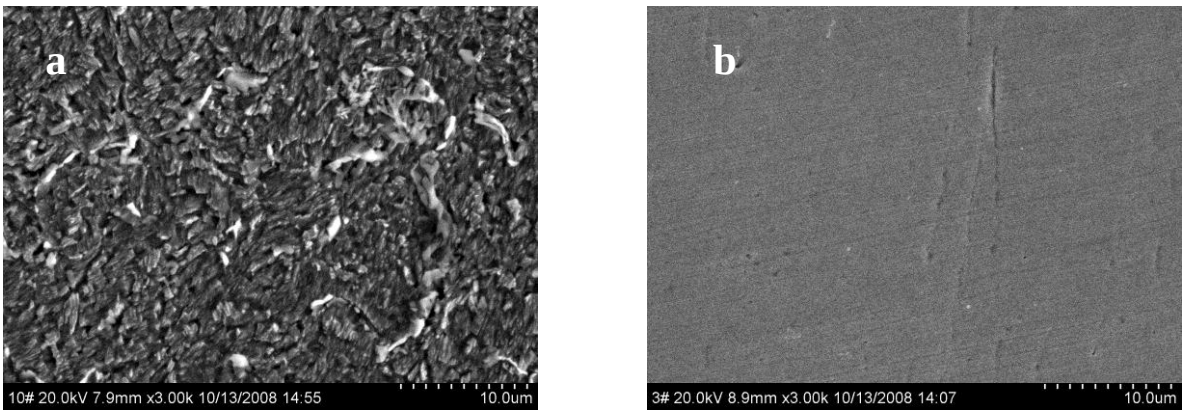

Figure 6. Micrographs of mild steel surface after immersion in 0.5 M HCl solution without inhibitor (a) and with addition of 0.16 mM BBMB (b).

As it is shown in Fig. 6a, the mild steel surface appears to be roughened extensively in the absence of inhibitor due to mild steel dissolution in corrosive solution. The surface is highly porous. The large and deep holes appear. However, the appearance of mild steel surface is significantly different after the addition of inhibitor to the 0.5 M HCl solution. It can be seen from Fig. 6b the smooth surface appears by formation of a protective film on the mild steel surface. This indicates that BBMB hinders the dissolution of iron and thereby reduces the rate of corrosion. This result could support high inhibition efficiency of BBMB.

4. CONCLUSIONS

The main conclusions of the present study could be drawn as the following points:

1. BBMB has shown a strong inhibitive effect for the corrosion of mild steel in 0.5 M HCl solution. The high inhibition efficiency (%) can be attributed to strong adsorption ability of BBMB molecules on mild steel surface. The inhibition efficiency increases with the increase in inhibitor concentration. The inhibitor showed maximum inhibition efficiency 92.6% at 0.16 mM concentration.

2. Potentiodynamic polarization studies showed that BBMB suppresses both anodic and cathodic process and thus acts as a mixed-type inhibitor. A very good agreement is obtained by weight loss measurements, potentiodynamic polarization and electrochemical impedance spectroscopy techniques.

3. The adsorption of BBMB was successfully described by the Langmuir adsorption isotherm. The corresponding adsorption free energy value demonstrated that the BBMB adsorption is a highly spontaneous process and chemisorption through electron transfer to form coordination bonds.

4. SEM observations of the electrode surface showed that a film of inhibitor molecules is formed on the electrode surface to retard both the reduction of hydrogen ions and the anodic dissolution of mild steel.

References

1. M. A. Quraishi, F. A. Ansari, *J. Appl. Electrochem*., 36 (2006) 309-314.
2. R. Bostan, S. Varvara, L. Gaina, L. M. Muresan, *Corros. Sci.*, 63 (2012) 275-286.
3. S. S. Abd El Rehim, H. H. Hassan, M. A. Amin, *Mater. Chem. Phys*., 78 (2002) 337-348.
4. F. Bentiss, M. Traisnel, N. Chaibi, B. Mernari, H. Vezin, M. Lagrenee, *Corros. Sci*., 44 (2002) 2271-2289.
5. M. Lebrini, M. Lagrenee, H. Vezin, L. Gengembre, F. Bentiss, *Corros. Sci*., 47 (2005) 485-505.
6. E. A. Noor, A. H. Al-Moubaraki, *Mater. Chem. Phys*., 110 (2008) 145-154.
7. M. Gopiraman, P. Sakunthala, D. Kesavan, V. Alexramani, I. S. Kim, N. Sulochana, *J. Coat. Technol. Res*., 9 (2012) 15-26.
8. K. F. Khaled, *Electrochimica Acta*, 48 (2003) 2493-2503.
9. A. Popova, M. Christov, S. Raicheva, E. Sokolova, *Corros. Sci*., 46 (2004) 1333-1350.
10. G. Bereket, E. Hur, C. Ogˇretir, *Molecular Structure (Thochem*), 578 (2002) 79-88.
11. El Sayed H. El Ashry, Ahmed El Nemr, Samy A. Essawy, Safaa Ragab, *Prog. Org. Coat*., 61 (2008) 11-20.
12. J. Cruz, R. Martinez, J. Genesca, E. Garcia-Ochoa, *J. Electroana. Chem*., 566 (2004) 111-121.
13. I. B. Obot, N. O. Obi-Egbedi, *Corros. Sci*., 52 (2010) 657-660.
14. Jacinto Morales Roque, T. Pandiyan, J. Cruz, E. García-Ochoa, *Corros. Sci.*, 50 (2008) 614-624.
15. H. J. Guadalupe, E. G. Ochoa, P. J. Maldonado-Rivas, J. Cruz, T. Pandiyan, *J. Electroana. Chem*., 655 (2011)164-172.
16. J. Aljourani, M. A. Golozar, K. Raeissi, *Mater. Chem. Phys*., 121 (2010) 320-325.
17. J. Aljourani, K. Raeissi, M.A. Golozar, *Corros. Sci.*, 51 (2009) 1836-1843.
18. M. Benabdellah, A. Tounsi, K. F. Khaled, B. Hammouti, *Arab. J. Chem*., 4 (2011) 17-24.
19. F. Zhang, Y. M. Tang, Z. Y. Cao, W. H. Jing, Z. L. Wu, Y. Z. Chen, *Corros. Sci*., 61 (2012) 1-9.
20. B.V. A. Rao, M. Y. Iqbal, B. Sreedhar, Electrochimica Acta, 55 (2010) 620-631.
21. X. M. Wang, H. Y. Yang, F. H. Wang, *Corros. Sci*., 52 (2010) 1268-1276.
22. X. M. Wang, H. Y. Yang, F. H. Wang, *Corros. Sci.*, 53 (2011) 113-121.
23. X. M. Wang, H. Y. Yang, F. H. Wang, *Corros. Sci*., 55 (2012) 145-152.
24. X. M. Wang, H. Y. Yang, F. H. Wang, *Int. J. Electrochem. Sci*., 7 (2012) 2403-2415.
25. S. X. Zhang, Paint Coat. Industry, 35 (2005) 4-6 (in Chinese).
26. N. A. Negm, Y.M. Elkholy, M. K. Zahran, S. M. Tawfik, *Corros. Sci*., 52 (2010) 3523-3536.
27. K. Tebbji, N. Faska, A. Tounis, H. Oudda, M. Benkaddour, B. Hammouti, *Mater. Chem. Phys*., 106 (2007) 260-267.
28. O. Olivares-Xometl, N. V. Likhanova, M. A. Dominggues-Aguilar, E. Arce, H. Dorantes, *Mater. Chem. Phys.*, 110 (2008) 344-351.
29. A. M. Abdel-Gaber, M. S. Masoud, E. A. Khalil, E. E. Shehata, *Corros. Sci.*, 51 (2009) 3021-3024.
30. M. S. Morad, A. M. Kamal El-Dean, *Corros. Sci*., 48 (2006) 3398-3412.
31. X. H. Li, G. N. Mu, *Appl. Surf. Sci*., 252 (2005) 1254-1265.
32. S. Issaadi, T. Douadi, A. Zouaoui, S. Chafaa, M. A. Khan, G. Bouet, *Corros. Sci.*, 53 (2011) 1484-13488.
33. G. Achary, H. P. Sachin, Y. Arthoba Naik, T. V. Venkatesha, *Mater. Chem. Phys*., 107 (2008) 44-50.
34. N. Z. N. Hashim, K. Kassim, Y. Mohd, APCBEE Procedia, 3 (2012) 239-244.
35. M. Vakili Azghandi, A. Davoodi, G.A. Farzi, A. Kosari, *Corros. Sci.*, 64 (2012) 44-54
36. M. Hosseini, SFL Merens, M, Ghorbani, *Mater. Chem. Phys*., 78(2003) 800-808.
37. K. F. Khaled, N. Hackerman, *Electrochim. Acta*, 48 (2003) 2715-2723.
38. E. Bayol, K. Kayakirilmaz, M. Erbil, *Mater. Chem. Phys.*, 104 (2007) 74-82.
39. L. Tang, G.. Mu, G.. Liu, *Corros. Sci*., 45 (2003) 2251-2262.
40. E. S. Ferreira, C. Giancomlli, F. C. Giacomlli, A. Spinelli, *Mater. Chem. Phys*., 83 (2004) 129-134.

41. L. j. M. Vračar, D. M. Dražić, *Corros. Sci*., 44 (2002) 1669-1680.
42. X. H. Li, S. D. Deng, *Corros. Sci*., 509 (2008) 420-430.
43. I. B. Obot, N. O. Obi-Egbedi, *Corros. Sci*., 52 (2010) 198-204.
44. S. Deng, X. Li, H. Fu, *Corros. Sci*., 52 (2010) 3840-3846.
45. F. S. Souza, A.Spinell, *Corros. Sci*., 51 (2009) 642-649.
46. K.C. Emreg, O. Atakol, *Mater. Chem. Phys*., 83 (2004) 373-379.
47. M. Behpour, S. M. Ghoreishi, N. Soltani, M. Salavati-Niasari, M. Hamadanian, A. Gandomi, *Corros. Sci*., 50 (2008) 2172-2181.
48. H. Ashassi-Sorkhabi, B. Shaabani, D. Seifzadeh, *Electrochim. Acta*, 50 (2005) 3446-3452.
49. M. Bouklah, B. Hammouti, M. Lagrenee, F. Bentiss, *Corros. Sci*., 46 (2006) 2831-2842.
50. B. G. Ateya, B. E. El-Anadouli, F. M. A. El-Nizamy, *Corros. Sci*., 24 (1984) 497-507.
51. M. Behpour, S. M. Ghoreishi, M. Salavati-Niasari, B. Ebrahimi, *Mater. Chem. Phys*., 107 (2008) 153-157.
52. R. Solmaz, E. Altunbas, G. Kardas, *Prot. Met. Phys. Met*., 47 (2011) 262-269.